Chemical Science

ROYAL SOCIETY OF CHEMISTRY

EDGE ARTICLE

View Article Online
View Journal | View Issue

Cite this: *Chem. Sci.*, 2022, **13**, 8618

All publication charges for this article have been paid for by the Royal Society of Chemistry

Carbocation catalysis in confined space: activation of trityl chloride inside the hexameric resorcinarene capsule†

Margherita De Rosa, *[a] Stefania Gambaro,[a] Annunziata Soriente,[a] Paolo Della Sala,[a] Veronica Iuliano,[a] Carmen Talotta,[a] Carmine Gaeta,[a] Antonio Rescifina *[b] and Placido Neri*[a]

Received 24th May 2022
Accepted 6th June 2022

DOI: 10.1039/d2sc02901d

rsc.li/chemical-science

Carbocation catalysis can be performed inside the confined space of the hexameric resorcinarene capsule. The inner cavity of the capsule can host the trityl carbocation, which catalyses the Diels–Alder reaction between dienes and unsaturated aldehydes. Experimental results and *in silico* calculations show that the hexameric resorcinarene capsule $\mathbf{C_6}$ can promote the formation of the trityl carbocation from trityl chloride through the cleavage of the carbon–halogen bond promoted by OH···X$^-$ hydrogen bonding. Here it is shown that the combination of the nanoconfined space and the latent carbocation catalysis provides a convenient complementary strategy for the typical carbocation catalysis. The latent strategy bypasses the typical pitfalls associated with active carbocations and provides control of the reaction efficiency in terms of reaction rate, conversion, and selectivity.

1. Introduction

Carbocations are relatively common species, generally unstable and non-isolable intermediates in several fundamental organic transformations and relevant industrial processes.[1] However, stable enough carbocations can also be obtained by an appropriate substitution around the carbocationic center with suitable stabilizing groups.[2] Classical carbocations are trivalent, planar species also called carbenium ions, whereas non-classical carbonium ions contain carbon centres with tetra-, penta-, or even higher coordination.[3]

Because of their positive charge, both carbenium and carbonium ions have been involved in catalytic systems.[4,5] In particular, carbenium ions (*e.g.*, triarylmethylium or trityl cations) have been used as highly efficient and highly versatile Lewis acid catalysts in a range of transformations, including Diels–Alder cycloaddition,[6] Mukaiyama aldol reaction,[7] Sakurai allylation,[8] Michael reaction,[9] halogenation,[10] epoxide rearrangement,[4b] hetero-ene cyclization,[4b] and oxo-metathesis.[11]

In recent years, several research groups have focused their attention on the hexameric capsule $(\mathbf{1})_6\cdot 8H_2O$ ($\mathbf{C_6}$), initially reported by Atwood,[12] which is obtained by self-assembly of six resorcinarene **1** units and eight water molecules (Fig. 1). $\mathbf{C_6}$ has been largely exploited as a nanoreactor[13] thanks to its ability to selectively host a wide range of substrates and to accelerate some organic reactions with excellent chemo-, regio-, and stereoselectivity. One advantage of using $\mathbf{C_6}$ as a nanocontainer is that its large cavity (internal volume of 1375 Å^3) can be easily engineered by introducing specific artificial cofactors.[14] In addition, the π-electron-rich cavity of $\mathbf{C_6}$ shows a high affinity for cationic species, which are stabilized by cation–π interactions.[13] For this reason, the $\mathbf{C_6}$ capsule behaves as a good catalyst for organic reactions involving cationic intermediates and/or transition states, which are shielded from chemical

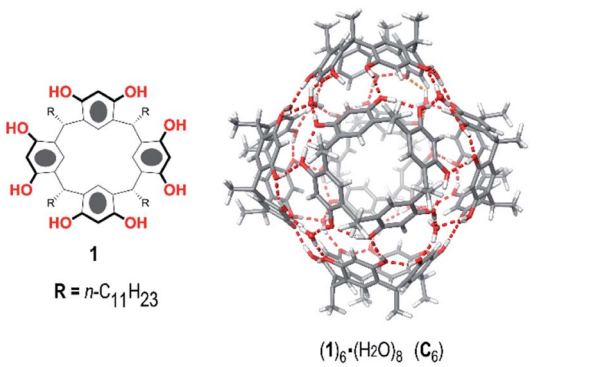

Fig. 1 Chemical drawing of *C*-undecylresorcin[4]arene **1** (left) and a reduced model (R = Me) of the hexameric capsule $(\mathbf{1}_R)_6\cdot(H_2O)_8$ ($\mathbf{C_6}$) (right).

[a]*Laboratory of Supramolecular Chemistry, Dipartimento di Chimica e Biologia "A. Zambelli", Università di Salerno, Via Giovanni Paolo II, I-84084, Fisciano (SALERNO), Italy. E-mail: maderosa@unisa.it; neri@unisa.it*

[b]*Dipartimento di Scienze del Farmaco e della Salute, Università di Catania, viale Andrea Doria, 6, 95125 Catania, Italy. E-mail: arescifina@unict.it*

† Electronic supplementary information (ESI) available: Full experimental procedures, *in silico* study, and characterisation for all compounds. See https://doi.org/10.1039/d2sc02901d

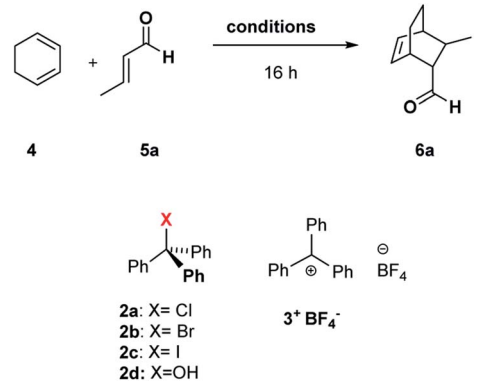

Scheme 1 Diels–Alder reaction between 1,3-cyclohexadiene **4** and crotonaldehyde **5a** in the presence of trityl chloride **2a** and the C_6 capsule.

quenching. In this way, interesting reactions involving cyclase mimics,[15] iminium catalysis,[14] Brønsted acid catalysis,[16] H-bond catalysis,[17] and halogen-bond catalysis[18] have been performed in the confined space of a C_6 capsule, frequently giving different outcomes with respect to the bulk medium. Another interesting catalysis performed inside the hexameric capsule was a mild Friedel–Crafts alkylation of (hetero)arenes in which C_6 acts as a Lewis acid catalyst by activating the C–Cl bond of benzyl chloride through H-bonding interactions.[19]

Based on these considerations, the question arises as to whether the hexameric C_6 capsule is also capable of carbocation catalysis with stable carbenium ions such as trityl cations: can trityl cations be hosted inside C_6 to achieve catalysis?

Can C_6 act as a Lewis acid catalyst by activating the less expensive trityl chloride (TrCl, **2a**, Scheme 1) as the carbocation source?

2. Results and discussion

Initially, we investigated the uptake of trityl chloride **2a** by C_6, in water-saturated $CDCl_3$ as the solvent, in order to form the capsule. Interestingly, upon adding **2a** to a C_6 solution, a red-orange color developed (see ESI Fig. S1†), indicative of the formation of the trityl cation (Tr^+, 3^+). This was confirmed by an absorption band at 424 nm in the UV-vis spectrum (Fig. S2 and S3†). The occurrence of such a combination band instead of the typical twin absorption band reported for the carbocation[20a] could be attributed to the electronic interactions between the phenyl rings of trityl cation and the aromatic walls of the capsule.[20b] The formation and encapsulation of 3^+ by C_6 was also demonstrated by 1D and 2D NMR studies (see the ESI†). An HSQC spectrum provided compelling evidence for the up-field shifted resonances of *o*-, *m*-, and *p*-H of the encapsulated Tr^+ cation (Fig. S14–S16†). In detail, the 2D HSQC spectrum of the mixture TrCl/C_6 in $CDCl_3$ showed relevant ^1J correlations at 7.12/128.9, 6.85/142.2, and 4.70/140.9 ppm attributable to encapsulated 3^+. Independent proof of the capability to encapsulate Tr^+ by C_6 was obtained by adding the trityl tetrafluoroborate salt $3^+\cdot BF_4^-$ to its water-saturated $CDCl_3$ solution. Also in this case, a similar red-orange color developed, and 1D and 2D NMR studies clearly showed the encapsulation of the Tr^+ cation inside the hexameric capsule C_6 (ESI, see Fig. S18–S22†). In detail, the 1D and 2D NMR spectra of the $C_6/3^+\cdot BF_4^-$ mixture (ESI†) showed a set of up-field shifted aromatic resonances (*o*-, *m*-, and *p*-H) of the encapsulated Tr^+ cation very similar to the signals observed upon mixing TrCl with C_6. Thus, the 2D HSQC experiment indicated the presence of ^1J correlations at 7.13/129.3, 6.83/141.4, and 4.75/141.0 ppm attributable to the encapsulated 3^+. Differently, the ^{1}H NMR spectrum of $3^+\cdot BF_4^-$ in dry $CDCl_3$ showed signals at 8.20 (*p*-H), 7.86 (*m*-H), and 7.70 (*o*-H). Another evidence came from the ^{13}C NMR spectrum of the mixture C_6/**2a** (Fig. S12 and S13†) which shows the presence of a characteristic up-field shifted $(Ph)_3C^+$ signal at 207.5 ppm. A very similar value (206.8 ppm) was observed in the ^{13}C NMR spectrum of the mixture $C_6/3^+\cdot BF_4^-$ (Fig. S20†), whereas the free salt $3\cdot BF_4^-$ gives an unshielded resonance at 211.3 ppm (Fig. S20†). Furthermore, DOSY NMR experiments performed on the mixtures C_6/**2a** (Fig. S17†) and **C6**/$3^+\cdot BF_4^-$ (Fig. S22†), showed that the signals of encapsulated 3^+ cation diffuse at the same rate as the capsule thus probing its internalization. In summary, all these data confirm that the C_6 capsule can act as a Lewis acid catalyst by activating trityl chloride **2a** to give the encapsulated carbocation $3^+@C_6$. At this point, we investigated the catalytic ability of the encapsulated triphenylmethylium $3^+@C_6$, obtained by mixing trityl chloride **2a** with C_6, in the Diels–Alder (DA) reaction between 1,3-cyclohexadiene **4** and crotonaldehyde **5a** (Scheme 1) in water-saturated $CDCl_3$ as the solvent. When the reaction mixture (Table 1, entry 1) was stirred at 30 °C for 16 h, adduct **6a** was obtained in 35% yield, whereas no product was obtained in the absence of **2a** (entry 2), C_6 (entry 3), or both (entry 4), thus confirming the crucial role played by the C_6 capsule as catalyst. The yield of **6a** was then increased to 92% by raising the temperature to 50 °C and using a **4**/**5a** ratio of 3 : 1 (Table 1, entry 6). With decreasing amount of **2a**, the reactivity slightly slowed down, showing a lower conversion to product **6a** after 16 h (Table 1, entry 7).

As concerns the stereochemistry of the DA reaction, in all instances, a high selectivity for *endo*-**6a** over *exo*-**6a** was observed with a ratio >99 : 1.

Table 1 Optimization of the reaction conditions for the Diels–Alder reaction between 1,3-cyclohexadiene **4** and crotonaldehyde **5a** in the presence of trityl chloride **2a** and the C_6 capsule

Entry[a]	*T* (°C)	**2a** (mol%)	Capsule (mol%)	**4** : **5a**	**6a** yield[b] (%)
1	30	26	26	1 : 1	35
2	30	—	26	1 : 1	—
3	30	26	—	1 : 1	—
4	30	—	—	1 : 1	—
5	50	26	26	1 : 1	50
6	50	26	26	3 : 1	92
7	50	10	26	3 : 1	80

[a] Reactions were performed on a 0.16 mmol scale using **4** (from 1 to 3 equiv.), **5a** (1 equiv.), **2a** (0.26 equiv.), and C_6 (0.26 equiv.) in 1.1 mL of water-saturated $CDCl_3$, for 16 h. [b] Isolated yield.

Table 2 Control experiments on the catalytic role of C_6 in the Diels–Alder reaction between 1,3-cyclohexadiene **4** and crotonaldehyde **5a**

Entry[a]	TrX	Additive[b] (equiv.)	**6a** yield[c] (%)	*endo* : *exo*[d]
1	–Cl	Et_4NBF_4 (10)	—	—
2	–Cl	DMSO (30)	—	—
3	BF_4^-	—	90	>99 : 1
4[e]	BF_4^-	—	43	>99 : 1
5	–Br	—	68	>99 : 1
6	–I	—	—	—
7	–OH	—	—	—

[a] Reaction conditions: **4** (0.45 M), **5a** (0.15 M), C_6 and TrX (0.039 M) in 1.1 mL of water-saturated $CDCl_3$, at 50 °C for 16 h. [b] Amount of additive with respect to C_6. [c] Isolated yield. [d] Determined by ^{1}H NMR analysis of the crude reaction mixture according to literature data.[21] [e] The reaction was performed in the absence of C_6.

The catalytic role played by the self-assembled resorcinarene capsule C_6 was corroborated by a series of control experiments (Table 2) in accord with a standard protocol previously described by us and others.[13–17] In particular, the DA reaction in Scheme 1 was performed in the presence of $Et_4N^+\cdot BF_4^-$ as a competitive guest for C_6,[13–17] and under these conditions, no hint of product **6a** was detected in the reaction mixture (Table 2, entry 1). Interestingly, under such conditions no red-orange colour develops (Fig. S36 and S37†) indicating the absence of encapsulated Tr^+ cation. On the other hand, in the presence of a very large quaternary ammonium cation (salt **14**, reported at pages S55 and S66†), too bulky to be accommodated within the cavity of C_6 (Fig. S23 and S24†), both the reaction (Fig. S39†) and the colour development (Fig. S38†) proceeded regularly. Furthermore, no hint of product **6a** was detected when the reaction in Scheme 1 was performed in the presence of hydrogen-bond competitor solvents (DMSO, Table 2, entry 2) able to disaggregate the capsule. These data strongly indicate that the reaction reported in Scheme 1 occurs in the nano-confined space inside the resorcinarene capsule C_6.

Previously,[19] we showed that the hexameric capsule C_6 was able to promote a Friedel–Crafts benzylation by a catalytically relevant H-bonding interaction between the bridged water molecules of the capsule and benzyl chloride, which was fundamental for the activation of the C–Cl bond in the substrate.[19] Based on these findings, we postulate that the bridged water molecules of the capsule C_6 establish an analogous H-bonding interaction, Tr–Cl···H–OH (C_6), that is fundamental for the activation of the C–Cl bond of **2a** and the formation of the trityl cation (Tr^+, $\mathbf{3}^+$) (*vide infra*, Fig. S78†).

To corroborate the catalytic role of this H-bonding interaction, we studied the reaction in Scheme 1 using trityl halides (TrX, X = Br and I) with halogen atoms of different H-bonding acceptor abilities. Interestingly, when **4** was reacted with **5a** in the presence of hexameric capsule C_6 and trityl bromide **2b**, product **6a** was obtained with a lower yield (68% yield, Table 2, entry 5), while no conversion to **6a** was observed in the presence of trityl iodide **2c** because the iodine atom in **2c** is a weaker H-bond acceptor.[22] Analogously, no hint of product **6a** was observed performing the reaction in Scheme 1 in the presence of trityl alcohol **2d** as the cofactor (Table 2, entry 7). These results clearly indicated that the C_6 capsule is more effective in abstracting the chloride anion over the bromide and iodide anions from the corresponding trityl halide, whereas it is incapable of detaching the OH group. Entries 3 and 4 in Table 2 clearly show that C_6 is catalytically active also in the presence of a preformed trityl cation, such as in salt $\mathbf{3}^+\cdot\mathbf{BF_4}^-$. In fact, this salt was an active catalyst by itself (43% yield, Table 2, entry 4), but gave superior performances in the presence of the C_6 capsule (90% yield, Table 2, entry 3).

Table 3 Scope study in the DA reaction of **4** and different dienophiles **5a–k**

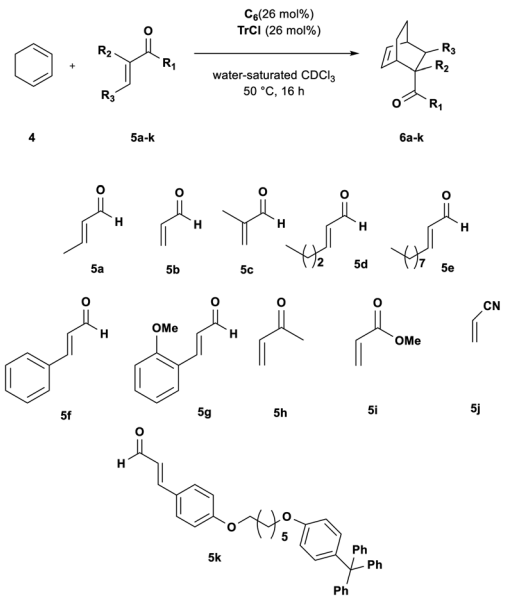

Entry[a]	**5**	Conv.[b] (%)	**6** yield[c] (%)	*endo* : *exo*[d]
1	**5a**	100	92	>99 : 1
2	**5b**	100	85	>99 : 1
3	**5c**	100	88	>99 : 1
4	**5d**	78	72	>99 : 1
5	**5e**	47	46	>99 : 1
6	**5f**	55	47	>99 : 1
7	**5g**	67	67	>99 : 1
8	**5h**	100	87	>99 : 1
9	**5i**	—	—	—
10	**5j**	—	—	—
11	**5k**	—	—	—

[a] Reaction conditions: **4** (0.45 M), **5** (0.15 M), C_6 and TrCl (0.039 M) in 1.1 mL of water-saturated $CDCl_3$, at 50 °C for 16 h. All aldehydes showed no background reaction in the absence of C_6 and **TrCl** under reaction conditions. [b] Determined by ^{1}H NMR analysis of the crude reaction mixture. [c] Isolated yield. [d] Determined by ^{1}H NMR analysis of the crude reaction mixture according to literature data.[21]

At this point, we investigated the substrate scope of the DA reaction promoted by C_6 exploring a variety of carbonyl compounds (Table 3). Under the standard reaction conditions, the procedure proved to be compatible with most structurally distinct substrates, affording the corresponding products in moderate to high yields. The reaction of both aldehydes **5a** and

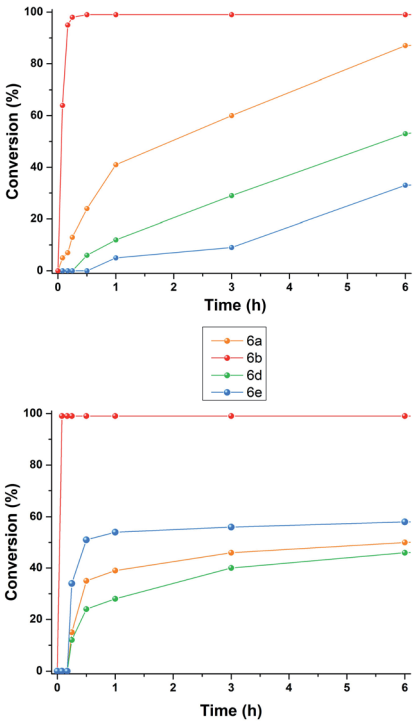

Fig. 2 Reaction progress for DA reaction between **4** and aldehydes **5a–e** in the presence of: (top) **2a** (26 mol%) and (26 mol%); (bottom) $3^{+}\cdot BF_4^{-}$.

5c with diene **4** to give the products **6a** and **6c** in the presence of the capsule was slower than the reaction of acrolein **5b** (see also Fig. 2), but at prolonged reaction time, all of them reached full conversion and no evidence of diene decomposition was detected.[4a]

Interestingly, the data reported in Table 3 clearly showed that the efficiency of the DA reaction between **4** and enals **5a–j** in the presence of $\mathbf{C_6}$ depended on the length of the R_3 alkyl chain in their β-position.

In particular, as chain length increased from **5a** (R_3 = Me, Table 3, entry 1) to **5d** (R_3 = *n*-C_3H_9, Table 3, entry 4) and **5e** (R_3 = *n*-C_8H_{17}, Table 3, entry 5), the conversion to **6x** greatly decreased from 92 to 46%.

With these results in hand, we studied and monitored the DA reaction between cyclohexadiene **4** with aldehydes **5a**, **5d**, and **5e** in the presence of preformed trityl fluoroborate salt $\mathbf{3^{+}\cdot BF_4^{-}}$ without capsule $\mathbf{C_6}$ (Fig. 2, bottom). ^{1}H NMR analysis of DA reactions over time showed that the reactions catalyzed by the preformed trityl fluoroborate salt and in the absence of $\mathbf{C_6}$ led to the DA adducts **6a**, **6d**, and **6e**, in moderate and comparable yields after 16 h, regardless of the alkyl chain length of the R_3 substituent. On the other hand, in the presence of **2a** and $\mathbf{C_6}$, the adducts **6a** and **6d** were formed faster than **6e** (Fig. 2, top). These results confirm that the reaction occurs within the cavity of $\mathbf{C_6}$ and the nano-environment of the capsule is sensitive to the different steric dimensions of the aldehydes.

Probably, $\mathbf{C_6}$ imposes a barrier for the entrance of sterically hindered aldehydes, thus making their reaction relatively slow compared to the other ones. These results indicate that the capsule $\mathbf{C_6}$ is able to exert a substrate selectivity toward the substrates **5a**, **b**, **d**, and **e**.[13–17]

In fact, in agreement with these considerations, and with the results previously reported by Franzén and coworkers,[4] trityl cation is temperature, air-, and moisture-sensitive, consequently, when the DA reaction was performed in the presence of cyclohexadiene and larger aldehyde such as **5d** and **5e**, which show slower kinetic of complexation inside **C6**, then the diene decomposition is favoured thus stopping the DA reaction and resulting in lower conversions. In fact, when only cyclohexadiene is added to a solution of trityl cation in dichloromethane complete decomposition or polymerization of the diene is observed.[4] In summary, under our reaction conditions, once trityl cation is formed from TrCl inside **C6**, if the aldehyde had kinetic difficulty getting into the capsule, then after prolonged reaction times we observed full consumption of the diene by its polymerization and the appearance of trityl alcohol. In addition, it is interesting to highlight that the encapsulated carbocation derived from $\mathbf{2a@C_6}$ was also effective for less-activated cinnamic aldehydes **5f** and **5g**, under the general

Table 4 DA reaction between 2,3-dimethylbutadiene **7** and various dienophiles

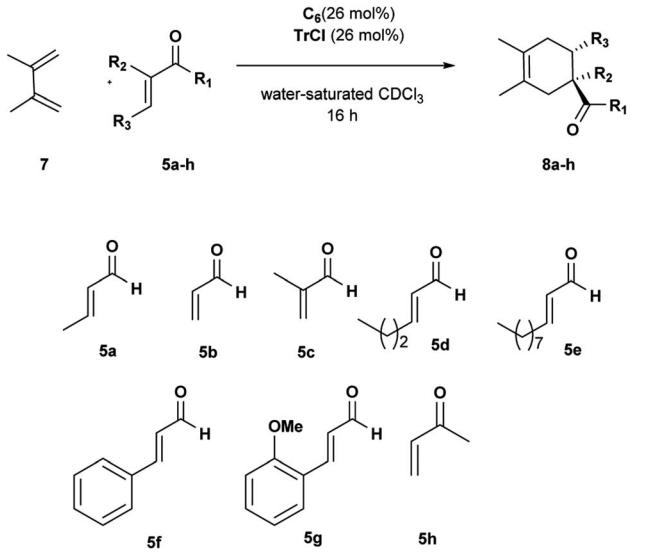

Entry[a]	5	Conv.[b] (%)	8 yield[c] (%)
1	**5a**	82	75
2	**5b**	100	82
3	**5c**	80	73
4	**5d**	32	27
5	**5e**	7	5
6	**5f**	16	16
7[d]	**5f**	34	27
8	**5g**	61	60
9	**5h**	100	92

[a] Reaction conditions: **7** (0.45 M), **5** (0.15 M), $\mathbf{C_6}$ and TrX (0.039 M) in 1.1 mL of water-saturated $CDCl_3$, at rt for 16 h. [b] Determined by ^{1}H NMR analysis of the crude reaction mixture according to literature data.[21a,b,26] [c] Isolated yield. [d] The reaction was carried out at 50 °C.

reaction conditions, affording the corresponding cycloadducts in moderate yields (Table 3, entries 6 and 7). The reaction of cinnamic aldehydes with cyclohexadiene **4** is not easy; different unsuccessful attempts have been reported in the literature characterized by the formation of complex mixtures of by-products due to the diene decomposition or polymerization.[23,24] Furthermore, Franzén and coworkers reported that the reaction does not work in the presence of preformed trityl fluoroborate salt $\mathbf{3}^{+}\cdot\mathbf{BF_4}^{-}$,[4a] but it is necessary to use a less active and more stable trityl cation, such as $(p\text{-MeOPh})_3CBF_4$, in order to obtain the adducts in moderate yield.

In our case, the $\mathbf{C_6}$ capsule can gradually provide the trityl carbocation in the reaction mixture *in situ*, thus avoiding diene side-reactions due to too long reaction times with less reactive dienophiles and tuning the Lewis acid properties of the trityl cation catalyst according to the reactivity of substrates. However, in accordance with literature data,[4a] the reaction failed with dienophiles such as acrylonitrile and methyl acrylate.

To extend the scope of our system, we carried out further studies with two other dienes with different reactivity,[25] such as open diene 2,3-dimethylbutadiene **7** and cyclopentadiene **9**.

The reactions with diene **7** proved to be more sensitive than those with diene **4** to the size of aldehydes.

The DA reactions with aldehydes **5a–c** afforded the corresponding adducts in high yields and selectivity just running at room temperature (Table 4, entries 1–3). A significant drop in reactivity was observed with sterically hindered aldehydes accompanied by a total consumption of more reactive diene **7** through polymerization (Table 4, entries 4–8). Increasing the reaction temperature and prolonging the reaction time did not improve the reaction efficiency. Interestingly, the corresponding reaction with OMe *ortho*-substituted cinnamic aldehyde **5g** led to better conversion, probably because it is preferentially encapsulated inside $\mathbf{C_6}$. Uptake NMR studies clearly showed that **5g** is encapsulated inside $\mathbf{C_6}$ to a greater extent than **5f**, and consequently, higher efficiency was observed for the conversion of **5g** in the product (see Fig. S25–S32†). We also examined the reaction with α,β-unsaturated ketone **5h**. Methyl vinyl ketone **5h** showed a reactivity comparable with acrolein, and the desired cycloadduct was afforded quantitatively (Table 4, entry 9).

Changing the diene to more reactive cyclopentadiene **9** had a significant influence on the rate and efficiency of the reaction. Aldehydes **5a–c** all reached full conversion in 1 h (Table 5,

Table 5 DA reaction between cyclopentadiene **5** and various dienophiles

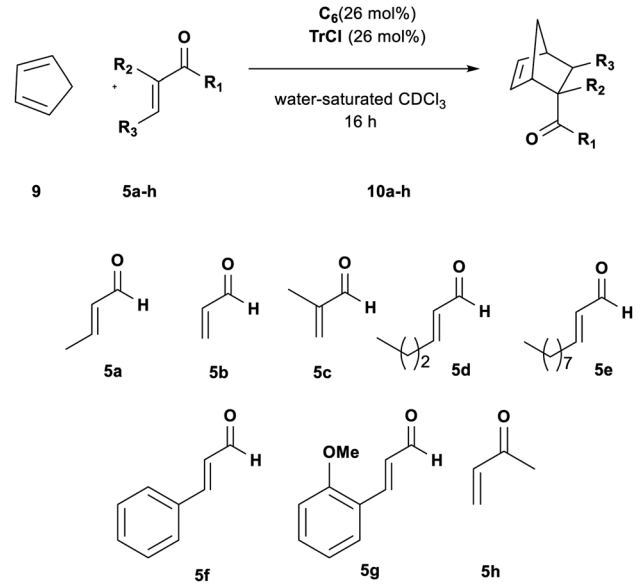

Entry[a]	5	*t* (h)	Conv.[b] (%)	**10** yield[c] (%)	*endo* : *exo*[d]
1	**5a**	1	100	90	86 : 14
2[e]	**5a**	1	—	—	—
3	**5b**	1	100	Quant	86 : 14
4[e]	**5b**	1	9	—	—
5[e]	**5b**	3	33	27	77 : 23
6	**5c**	1	100	Quant	2 : 98
7	**5d**	4	94	90	69 : 25
		16	100	96	77 : 23
8	**5e**	4	78	72	84 : 16
		16	95	91	84 : 16
9	**5f**	4	54	50	91 : 9
		16	72	68	89 : 11
10	**5g**	4	37	34	84 : 16
		16	61	60	80 : 20
11	**5h**	2	Quant	93	>99 : 1

[a] Reaction conditions: **9** (0.45 M), **5** (0.15 M), $\mathbf{C_6}$ and **TrCl** (0.039 M.) in 1.1 mL of water-saturated $CDCl_3$, at rt. [b] Determined by ^{1}H NMR analysis of the crude reaction mixture. [c] Isolated yield. [d] Determined by ^{1}H NMR analysis of the crude reaction mixture according to literature data.[21b,21d,27] [e] The reaction was performed in the absence of $\mathbf{C_6}$ and **TrCl**.

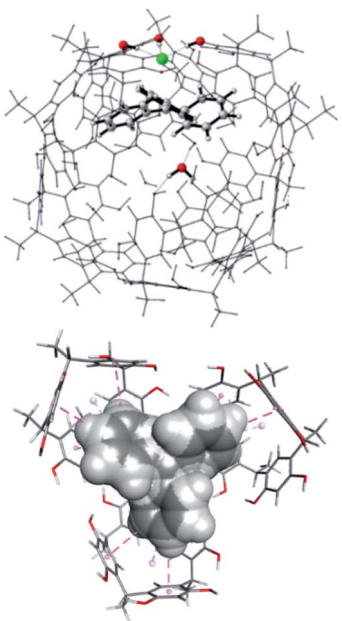

Fig. 3 The most stable structure of ionized trityl chloride inside the hexameric resorcinarene capsule ($Tr^{+}\cdot Cl^{-}$@CM). (Top) Balls and sticks refer to the QM level. (Bottom) Bottom view regarding the plane that cuts the capsule parallel to the trityl cation longitudinal axes; the dots and dashed-lines in purple refer to CH–π interactions.

entries 1, 3 and 6); by increasing the size of the R_3 group in aldehydes **5d** and **5e** a size selectivity could be initially detected but extending the reaction time to 16 h the adducts were obtained in high conversion for both aldehydes (Table 5, entries 7 and 8).

Thus, we subsequently evaluated the reaction with cinnamic aldehydes **5f** and **5g**. In a similar fashion to the reaction with **4**, both substrates gave the target products in satisfactory yields confirming the feasibility of the reaction (Table 5, entries 9 and 10). Finally, also ketone **5h** was found to be a very good dienophile for this reaction giving cycloadduct **8h** in high yield (Table 5, entry 11).

To further investigate the reaction mechanism that leads to the peculiar catalytic role played by the hexameric capsule $\mathbf{C_6}$ (Scheme 1), we conducted an *in silico* study by employing both molecular dynamics (MD) simulations and quantum-mechanical (QM) investigations.

In this last case, we employed a reduced model capsule CM assembled with the *C*-methylresorcinarene and the ONIOM method. Initially, to corroborate our findings on the catalytic role of the capsule as a Lewis acid, we studied the encapsulation of trityl chloride **2a** and its ionized form to give the ($Tr^+ \cdot Cl^- @ C_M$) complex. Interestingly, in the most stable structure of $\mathbf{2a@C_M}$ (Fig. S78†), the chlorine atom of **2a** engages a hydrogen bond with a structural water molecule, which weakens the C–Cl bond making it significantly longer.

The most stable structure of the $Tr^+ \cdot Cl^- @ C_M$ complex was found through an MD study of 2 μs, at the molecular mechanics (MM) level with chloroform as the explicit solvent, starting from the structure with the trityl carbocation inside the capsule and the chloride anion outside, near a structural water molecule. Finally, the most stable structure obtained by analyzing the MD trajectory was more stable than the reagents ($\Delta G = -1.14$ kcal mol^{-1}), showing the peculiarity of possessing the chloride anion replacing a structural water molecule.[28] The replaced H_2O molecule was anchored to the internal wall of the capsule through two hydrogen bonds with another structural water molecule and an oxygen atom of a resorcinol moiety (Fig. 3, top).

Table 6 Relative Gibbs free energy of inclusion (ΔG) and electrophilicity index (ω)

Compound	ΔG inclusion[a] (kcal mol^{-1})	ω (eV)
TrF	—	1.11
TrCl	—	1.17
TrBr	—	1.31
TrI	—	1.52
$TrBF_4$	—	3.48
$\mathbf{TrF@C_M}$	9.81	3.29
$\mathbf{TrCl@C_M}$	−1.14	3.16
$TrBr@C_M$	−3.20	3.29
$TrI@C_M$	−2.41	3.46
$\mathbf{TrBF_4@C_M}$	−8.86	3.69

[a] Referring to those of the host and the corresponding non-encapsulated guests.

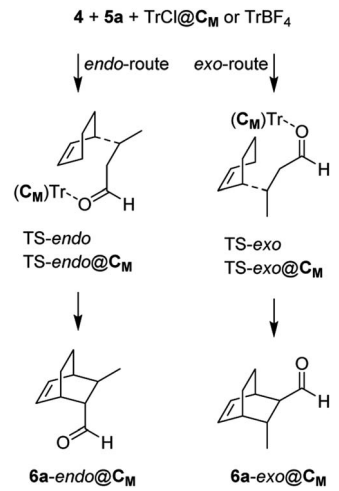

Scheme 2 *Endo* and *exo* routes for the *in silico* studies of the model DA reactions and nomenclature adopted: TS-*endo* and TS-*exo* refer to the reaction with $TrBF_4$, while TS-*endo*@$\mathbf{C_M}$ and TS-*exo*@$\mathbf{C_M}$ refer to the reaction with TrCl and the capsule.

In this structure, the trityl cation is in its catalytically active form and is nested in one side of the capsule with its three phenyl rings pointing towards the inner cavity of three resorcin[4]arene macrocycles (Fig. 3, bottom) and establishing stabilizing CH–π and π–π interactions.

MD simulations with the other trityl halides and $TrBF_4$ brought approximatively the same structure obtained with the chloride anion.

The Gibbs free energy of inclusion (ΔG) and the electrophilicity index (ω) of the investigated compounds are reported in Table 6. Except for TrF, all other trityls easily enter into the capsule, and the electrophilicity indexes of their complexes are comparable to that of free $TrBF_4$, indicating that they can behave as Lewis acids (in contrast, the electrophilicity indexes of all free trityl halides are in the range of 1.11–1.52, indicating that they are poor electrophiles).

The explanation of the different reactivity observed for TrX (X = Cl, Br, I, BF_4) comes from the MD studies. All $TrX@C_M$ complexes, starting with the counterion of the trityl outside the capsule, incorporate the anion within 2 ns in the position previously occupied by a structural water molecule, with the exception of iodide that employs about 80 ns. Interestingly, $TrCl@C_M$ and $TrBF_4@C_M$ complexes remain stable for the entire simulation period (2 μs), whereas $TrBr@C_M$ and $TrI@C_M$ become unstable at around 50 and 82 ns (just 2 ns after acquiring the adequate catalytic power), respectively, and then the network of hydrogen bonds begins to falter, leading to the opening of the capsule. This is ideally in accordance with the high yields observed for X = Cl and BF_4, and for the moderate yield obtained with X = Br. In the case of X = I, the complex collapses very quickly and does not give rise to the cycloaddition reaction. Subsequently, we studied, at the QM/SE level, the DA reaction inside the capsule using as a model reaction the $TrCl@C_M$ complex, cyclohexa-1,3-diene **4**, and (*E*)-crotonaldehyde **5a**. At the same time, we investigated the same reaction using $TrBF_4$ in the absence of the capsule (Scheme 2). The

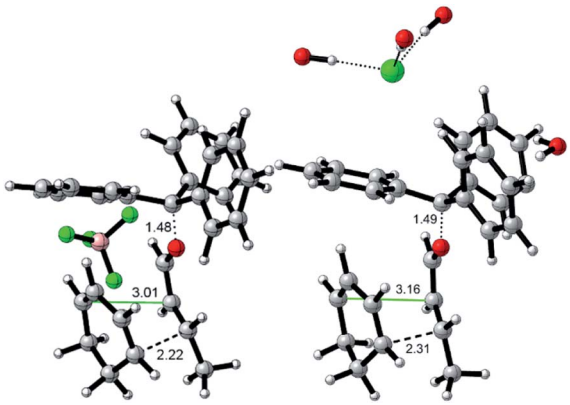

Fig. 4 Geometries for the most energetically favored TS-*endo* (DA with $TrBF_4$ without the capsule, left) and TS-*endo*@$\mathbf{C_M}$ (DA with TrCl and the capsule, right) routes (only at the QM level). Lengths are in Å. Carried out with CYLview.[29]

Table 7 Relative Gibbs free energies (ΔG, in kcal mol^{-1}) and transferred charges (e, in a.u.) for the species depicted in Scheme 2

Species	ΔG^a	$q_{CT}{}^b$ (e)
TS-*endo*	13.43	0.62
TS-*exo*	16.06	0.81
TS-*endo*@$\mathbf{C_M}$	17.58	0.16
TS-*exo*@$\mathbf{C_M}$	20.17	0.27
6-*endo*@$\mathbf{C_M}$	−6.12	—
6-*exo*@$\mathbf{C_M}$	−6.20	—

[a] Referring to those of the host and the corresponding non-encapsulated guests. [b] In terms of the residual charge of the diene **4** fragment in the transition state.

relative Gibbs free energies and the transferred charges for the species depicted in Scheme 2 are reported in Table 6, whereas all energetic parameters are given in Table S1.† The *endo*/*exo* TS energy difference in both reactions is high (2.59 and 2.63 kcal mol^{-1}) and in accordance with the experimentally observed *endo*/*exo* ratio.

Although the TS energy barrier is highest for the reaction inside the capsule (and this justifies the improvement of the yield observed at 50 °C), the yield and the course of the reaction worsen in its absence (*vide infra* for a possible explanation). In both the model reactions, we were unable to locate a concerted transition state due to the high positive charge that develops on the carbon beta to the dienophile during its complexation with the trityl carbocation. Effectively, the DA reactions at hand proceed with a stepwise mechanism in which the first step consists of a Michael-type addition of the diene to the β-carbon of the dienophile, whereas in the second one, barrierless in a vacuum, the reaction proceeds by joining the two carbon atoms bearing the developing opposite partial charges.

Interestingly, the two reactions proceed with a different geometry arrangement with respect to the trityl carbocation and the respective counteranions, as depicted in Fig. 4 that report the 3D structures of TS-*endo* and TS-*endo*@$\mathbf{C_M}$.

This behavior could justify the differences in the efficiency of the reactions with $TrBF_4$ without and with the capsule. When BF_4^- is from the same side of the diene and the dienophile probably hinders the progress of the reaction. In contrast, the presence of the capsule precludes the possibility of making the reaction take place from the same side of the anion, as the space is not enough. Moreover, in this last case, the trityl cation is firmly anchored thanks to the phenyls that point inside the cavity of the resorcinarenes and, under these conditions, its electrophilicity index increase by 0.21 eV (Table 6). Noteworthily, the structural water molecule that in TrCl@$\mathbf{C_M}$ was anchored to the capsule wall now has moved to the trityl cation and establishes two OH–π interactions with two phenyls, and in all TSs, the (*E*)-crotonaldehyde is in *s-cis* conformation (Fig. 4, right). Finally, both the TS-*endo* and TS-*exo* are more advanced with respect to the corresponding TS-*endo*@$\mathbf{C_M}$ and TS-*exo*@$\mathbf{C_M}$, which is in accord with the lower charge transfer found in the latter (Table 7).

Presumably, the presence of the capsule and the displacement of the structural water molecule anchored to its internal wall towards the phenyls of trityl mitigates the ionicity of the transition state while failing to make the DA reaction concerted.

3. Conclusions

In conclusion, we have herein reported that the DA reaction can occur in the nanoconfined space of the hexameric resorcinarene capsule $\mathbf{C_6}$, and the capsule is able to promote the reaction through the activation of the dienophile by a carbocation catalyst generated *in situ*. $\mathbf{C_6}$ can form an active trityl ion from TrCl as a carbocation precursor through the cleavage of the carbon–halogen bond promoted by OH···X^- hydrogen bonding. We believe that the combination of the nanoconfined space and the latent carbocation catalysis would provide a complementary strategy to the typical carbocation catalysis. The latent strategy bypasses the typical pitfalls associated with active carbocations and provides control of the reaction efficiency in terms of reaction rate, conversion, and selectivity.

Conflicts of interest

There are no conflicts to declare.

Acknowledgements

The authors acknowledge the Regione Campania (POR CAMPANIA FESR 2007/2013 O.O.2.1, CUP B46D14002660009) for the FT-ICR mass spectrometer facilities and the "Centro di Tecnologie Integrate per la Salute" (CITIS) (project PONa3_00138) for the 600 MHz NMR facilities. Financial support from the University of Salerno (FARB) is acknowledged.

Notes and references

1 G. A. Olah, *Angew. Chem., Int. Ed.*, 1995, **34**, 1393–1405.
2 M. Horn and H. Mayr, *J. Phys. Org. Chem.*, 2012, **25**, 979–988, and references therein.
3 G. A. Olah, *J. Am. Chem. Soc.*, 1972, **94**, 808–820.

4 (*a*) J. Bah and J. Franzén, *Chem.–Eur. J.*, 2014, **20**, 1066–1072; (*b*) J. Bah, V. R. Naidu, J. Teske and J. Franzén, *Adv. Synth. Catal.*, 2015, **357**, 148–158; (*c*) V. R. Naidu, J. Bah and J. Franzén, *Eur. J. Org. Chem.*, 2015, **2015**, 1834–1839; (*d*) V. R. Naidu, S. Ni and J. Franzén, *Chem. Cat. Chem.*, 2015, **7**, 1896–1905.

5 (*a*) R. Properzi, P. S. J. Kaib, M. Leutzsch, P. Gabriele, M. Raja, C. K. De, L. Song, P. R. Schreiner and B. List, *Nat. Chem.*, 2020, **12**, 1174–1179; (*b*) X. Tang, W. Chen, X. Yi, Z. Liu, Y. Xiao, Z. Chen and A. Zheng, *Angew. Chem., Int. Ed.*, 2021, **60**, 4581–4587.

6 (*a*) A. Brunner, S. Taudien, O. Riant and H. B. Kagan, *Chirality*, 1997, **9**, 478–486; (*b*) S. Taudien, O. Riant and H. B. Kagan, *Tetrahedron Lett.*, 1995, **36**, 3513–3582; (*c*) S. Ni, V. R. Naidu and J. Franzén, *Eur. J. Org. Chem.*, 2016, **9**, 1708–1713; (*d*) Q. Zhang, J. Lv, S. Li and S. Luo, *Org. Lett.*, 2018, **20**, 2269–2272.

7 (*a*) S. Kobayashi, S. Murakami and T. A. Mukaiyama, *Chem. Lett.*, 1985, **14**, 447–450; (*b*) S. Kobayashi, M. Murakami and T. Mukaiyama, *Chem. Lett.*, 1985, **14**, 1535–1538; (*c*) S. E. Denmark and C.-T. Chen, *Tetrahedron Lett*, 1994, **35**, 4327–4330.

8 T. Mukaiyama, H. Nagaoka, M. Murakami and M. Ohshima, *Chem. Lett.*, 1985, **14**, 977–980.

9 S. Kobayashi, M. Murakami and T. Mukaiyama, *Chem. Lett.*, 1985, **14**, 953–956.

10 S. Ni, M. A. A. El Remaily and J. Franzén, *Adv. Synth. Catal.*, 2018, **360**, 4197–4204.

11 S. Ni and J. Franzén, *Chem. Commun.*, 2018, **54**, 12982–12985.

12 (*a*) L. R. MacGillivray and J. L. Atwood, *Nature*, 1997, **389**, 469–472; (*b*) A. Shivanyuk and J. Rebek, *J. Am. Chem. Soc.*, 2003, **125**, 3432–3433; (*c*) L. Avram and Y. Cohen, *Org. Lett.*, 2002, **4**, 4365–4368.

13 (*a*) D. Ajami and J. Rebek Jr, *Acc. Chem. Res.*, 2013, **46**, 990–999; (*b*) L. Catti, Q. Zhang and K. Tiefenbacher, *Chem.–Eur. J.*, 2016, **22**, 9060–9066; (*c*) G. Borsato, J. Rebek Jr and A. Scarso, in *Selective Nanocatalysts and Nanoscience Concepts for Heterogeneous and Homogeneous Catalysis*, ed. A. Zecchina, S. Bordiga and E. E. Groppo, Wiley-VCH Verlag GmbH & Co. KGaA, Weinheim, Germany, 2011, pp. 105–168; (*d*) L. Avram, Y. Cohen and J. Rebek Jr, *Chem. Commun.*, 2011, **47**, 5368–5375; (*e*) G. Borsato and A. Scarso, in *Organic Nanoreactors*, ed. S. Sadjadi, Academic Press, 2016, ch. 7, pp. 203–234; (*f*) L. Catti, T. Brauer, Z. Qi and K. Tiefenbacher, *Chimia*, 2016, **70**, 810–814; (*g*) Q. Zhang, L. Catti and K. Tiefenbacher, *Acc. Chem. Res.*, 2018, **51**, 2107–2114; (*h*) C. Gaeta, C. Talotta, M. De Rosa, P. La Manna, A. Soriente and P. Neri, *Chem.–Eur. J.*, 2019, **25**, 4899–4913; (*i*) C. Gaeta, P. La Manna, M. De Rosa, A. Soriente, C. Talotta and P. Neri, *Chem. Cat. Chem.*, 2020, **13**, 1638–1658; (*j*) C. Gaeta, C. Talotta, M. De Rosa, P. La Manna, A. Soriente and P. Neri, in *Reactivity in Confined Spaces*, ed. R. S. Forgan and G. O. Lloyd, The Royal Society of Chemistry, 2021, ch. 5, pp. 133–166.

14 (*a*) T. M. Bräuer, Q. Zhang and K. Tiefenbacher, *Angew. Chem., Int. Ed.*, 2016, **55**, 7698–7701; (*b*) P. La Manna, M. De Rosa, C. Talotta, C. Gaeta, A. Soriente, G. Floresta, A. Rescifina and P. Neri, *Org. Chem. Front.*, 2018, **5**, 827–837; (*c*) S. Gambaro, C. Talotta, P. Della Sala, A. Soriente, M. De Rosa, C. Gaeta and P. Neri, *J. Am. Chem. Soc.*, 2020, **142**, 14914–14923.

15 (*a*) Q. Zhang, J. Rinkel, B. Goldfuss, J. S. Dickschat and K. Tiefenbacher, *Nat. Catal.*, 2018, **1**, 609–615; (*b*) Q. Zhang and K. Tiefenbacher, *Angew. Chem., Int. Ed.*, 2019, **58**, 12688–12695.

16 (*a*) Q. Zhang and K. Tiefenbacher, *J. Am. Chem. Soc.*, 2013, **135**, 16213–16219; (*b*) J. M. Köster and K. Tiefenbacher, *Chem. Cat. Chem.*, 2018, **10**, 2941–2944.

17 (*a*) S. Gambaro, M. De Rosa, A. Soriente, C. Talotta, G. Floresta, A. Rescifina, C. Gaeta and P. Neri, *Org. Chem. Front.*, 2019, **6**, 2339–2347; (*b*) P. La Manna, C. Talotta, M. De Rosa, A. Soriente, C. Gaeta and P. Neri, *Org. Lett.*, 2020, **22**, 2590–2594.

18 P. La Manna, M. De Rosa, C. Talotta, A. Rescifina, G. Floresta, A. Soriente, C. Gaeta and P. Neri, *Angew. Chem., Int. Ed.*, 2020, **59**, 811–818.

19 P. La Manna, C. Talotta, G. Floresta, M. De Rosa, A. Soriente, A. Rescifina, C. Gaeta and P. Neri, *Angew. Chem., Int. Ed.*, 2018, **57**, 5423–5428.

20 (*a*) T. Shida in *Electronic Absorption Spectra of radical Ions*, Elsevier, Amsterdam, The Netherlands, 1988; (*b*) R. Rathore, C. L. Burns and I. A. Guzei, *J. Org. Chem.*, 2004, **69**, 1524–1530.

21 (*a*) Z. Zhu and J. H. Espenson, *J. Am. Chem. Soc.*, 1997, **119**, 3507–3512; (*b*) H. F. T. Klare, K. Bergander and M. Oestreich, *Angew. Chem., Int. Ed.*, 2009, **48**, 9077–9079; (*c*) R. K. Schmidt, K. Müther, C. Mück-Lichtenfeld, S. Grimme and M. Oestreich, *J. Am. Chem. Soc.*, 2012, **134**, 4421–4428; (*d*) E. Gould, T. Lebl, A. M. Z. Slawin, M. Reid, T. Daviesb and A. D. Smith, *Org. Biomol. Chem.*, 2013, **11**, 7877–7892.

22 G. R. Desiraju and T. Steiner, *The weak hydrogen bond: in structural chemistry and biology*, Oxford University Press, Oxford; New York, 1999.

23 A. C. Kinsman and M. Kerr, *Org. Lett.*, 2000, **2**, 3515–3520.

24 T. Arndt, P. K. Wagner, J. J. Koenig and M. Breugst, *Chem. Cat. Chem.*, 2021, **13**, 2922–2930.

25 (*a*) R. S. Paton, S. Kim, A. G. Ross, S. J. Danishefsky and K. N. Houk, *Angew. Chem., Int. Ed.*, 2011, **50**, 10366–10368; (*b*) B. J. Levandowski and K. N. Houk, *J. Org. Chem.*, 2015, **80**, 3530–3537.

26 (*a*) F. Fu, Y.-C. Teo and T.-P. Loh, *Org. Lett.*, 2006, **8**, 5999–6001; (*b*) E. Taarning and R. Madsen, *Chem.–Eur. J.*, 2008, **14**, 5638–5644.

27 (*a*) K. Ishihara, H. Kurihara, M. Matsumoto and H. Yamamoto, *J. Am. Chem. Soc.*, 1998, **120**, 6920–6930; (*b*) H. Gotoh and Y. Hayashi, *Org. Lett.*, 2007, **9**, 2859–2862; (*c*) H. He, B.-J. Pei, H.-H. Chou, T. Tian, W.-H. Chan and A. W. M. Lee, *Org. Lett.*, 2008, **10**, 2421–2424.

28 S. Merget, L. Catti, G. M. Piccini and K. Tiefenbacher, *J. Am. Chem. Soc.*, 2020, **142**, 4400–4410.

29 C. Y. Legault, *CYLview20*, Université de Sherbrooke, 2020, **http://www.cylview.org**.